Appl. Phys. A 79, 997–999 (2004)
DOI: 10.1007/s00339-004-2613-2

Applied Physics A
Materials Science & Processing

A.A. MOROZOV

Thermal model of pulsed laser ablation: back flux contribution

Institute of Thermophysics, Lavrentyev ave. 1, 630090, Novosibirsk, Russia

Received: 12 January 2004 / Accepted: 15 January 2004
Published online: 26 July 2004 •

ABSTRACT This paper proposes improvement of the boundary conditions for the thermal model of laser-induced solid heating and ablation. The refinement of the model takes into account the back flux from the vapor cloud to the evaporation surface. For a wide range of evaporation rates, the value of the back flux was determined by direct Monte Carlo simulation of vapor cloud expansion. The obtained back flux values are substituted to the thermal model. The improved model has been shown to be in good agreement with the experimental results on graphite as an example.

PACS 52.38.Mf; 79.20.Ds; 81.15.Fg

1 Introduction

Laser ablation of solids with nanosecond pulses of moderate intensity ($1–10\,J/cm^2$) is widely used in modern technologies, such as thin film deposition, surface treatment, cluster formation, etc. [1, 2]. Laser pulse action leads to formation of a vapor cloud of ablation products. To describe accurately the process of the cloud formation and expansion, it is necessary to know the mechanisms of interaction of laser radiation with matter.

Many works are deduced to describe laser radiation absorption in the target and in the forming cloud [3–8]. In these works, the one-dimensional problem of laser-induced solid heating is solved. Correct consideration of the boundary conditions at the evaporation surface is hampered by need to determine the mass and energy fluxes from the cloud back to the surface due to collisions of particles in the cloud.

The value of the back flux depends on the amount of evaporated matter and varies from zero for collisionless expansion at laser desorption to a value corresponding to stationary expansion into vacuum. However, in the majority of works, dependence of the back flux on evaporation rate is not taken into consideration. The back flux is either ignored completely [3–6] or set identical to that for stationary evaporation, i.e., 18–20% [7, 8].

✉ Fax: +7-3832/343-480, E-mail: morozov@itp.nsc.ru

Only in several works does the back flux correlate with the evaporation rate. In [9], for intense evaporation, when the expanding vapor can be considered as a continuum, the back flux is defined by the flow parameters at the Knudsen layer front, and for the whole range of evaporation rate an exponential dependence between the back flux and the vaporization velocity is taken. In [10], in the modeling of evaporation of two monolayers of graphite, the back flux value is found by solving of the conjugate problem of vapor cloud expansion by the method of direct Monte Carlo simulation.

The evaporated particles continue returning to the surface during a very prolonged time after pulse termination, and this leads to a considerable increase in the back flux. It was shown that for intense evaporation after evaporation termination, 10–43% of particles can return to the surface [11, 12]. Hence, the value of the back flux during pulse and after its termination can be appreciable, and its disregard can cause a considerable error. Furthermore, the energy of returning particles may be far less than the energy of evaporated particles, and this can cause an additional error.

The back flux contribution to the thermal model of pulsed laser ablation appears to be substantial and should be taken into consideration. However, at the present time, the data on the back flux value for the overall range of evaporation rate are very scanty. The back flux value may be determined by the method of direct Monte Carlo simulation [13]. This method was used widely for simulation both steady [14, 15] and pulsed [10, 16–19] evaporation into vacuum. However, in these works the dependence of back flux on evaporation rate was not studied.

This work presents results on the determination of the back flux as a function of the number of evaporated monolayers during evaporation and after its termination in a wide range of evaporation intensity, when the forming flow changes from collisionless to the continuum one. The obtained values are used in the thermal model of laser-induced target heating and evaporation. The importance of the back flux consideration is illustrated by the example of graphite.

2 Back flux determination by the direct Monte Carlo simulation of vapor cloud expansion

During pulse under the considered conditions of laser ablation (nanosecond pulse duration, laser radiation spot

diameter of order of 1 mm) cloud expansion is practically one-dimensional. Later the cloud begins extending transversally, implying two-dimensionality of the problem. Since our interest is limited by the determination of the total number of particles returning to the surface, whether to the irradiation spot or beyond it, one dimensional calculation can be used as a rough approximation.

The problem of particle evaporation from a surface with consequent expansion into vacuum is considered in a one-dimensional approach. Particles are evaporated according to the diffusive law with energy corresponding to the surface temperature T_S. During the time interval τ, particle flux Ψ is constant and equal to $\Psi = n_S u_T/4$, where n_S is the density of the saturated gas corresponding to the temperature T_S, $u_T = \sqrt{8kT_S/(\pi m)}$, m is the molecular mass, k is the Boltzmann constant. All backscattered particles recondense at the surface. A monatomic gas is considered. To describe particle interaction, the hard sphere model is used [13]. The only parameter of the problem is the number of evaporated monolayers $\Theta = \Psi\tau\Sigma$, where Σ is an area occupied by one particle at the surface.

A particular emphasis has been placed on the determination of the back flux value during time sufficient for the cloud to reach the substrate, i.e., the time that is much longer than pulse duration τ. In the simulation, cloud expansion was followed up during time interval of $10^7\tau$. During such a prolonged timespan, cloud expansion is characterized both by a considerable density decrease in the cloud core and by large parameter gradients at the cloud front. Therefore, an adaptive grid was used. The grid was built to limit the cell size to 0.25 of the local mean free path. For construction of such a grid, preliminary calculations with a small number of particles and a large time step were performed. Based on the calculations, the spatial density profiles in different time moments were estimated and used for building the adaptive grid. Number of particles in calculations was up to 5 000 000.

To test the program, calculations of stationary and pulsed evaporation into vacuum for conditions presented in works [14, 19] were carried out. The results were found to agree well with the data obtained in [14, 19].

Calculations were performed for the number of evaporated monolayers $\Theta = 10^{-3} - 10^{3}$. The time evolution of back flux β for different values Θ is presented in Fig. 1. At any time moment, β was defined as the ratio of the total number of recondensed particles to the total number of evaporated particles. It is seen that for any $\Theta > 1$, β tends to a common limiting value of about 27.5%. It is worth noting that the maximum value of back flux during pulse corresponds to the back flux at stationary evaporation of 16.3% [14]. After termination of evaporation, one can see a sharp increase of β due to stopping particle evaporation.

Particular attention was paid to the post-pulse back flux. The fraction of particles returned to the target after evaporation termination is defined as $\beta_{POST}(t) = \frac{\beta(t)-\beta(\tau)}{1-\beta(\tau)}$. Dependence of β_{POST} on the number of evaporated monolayers is not monotone with a maximum in the vicinity of $\Theta = 1$ (Fig. 2). The maximum is obviously caused by a small back flux during evaporation ($\beta = 6\%$) and a large back flux after its termination ($\beta = 27.2\%$) (Fig. 1).

Similar results for recondensed quantity were obtained in [11] based on analytical approximation under the assumption of continuum cloud expansion (i.e., $\Theta = \infty$), and in [12] based on numerical solution of the Boltzmann equation for $\Theta \approx 20$. For example, in [11] $\beta_{POST}(20\tau) = 8.9 \pm 1.66\%$, in [12] $\beta_{POST}(18\tau) \approx 10\%$, and in the present work for $\Theta = 1000$ we have $\beta_{POST}(20\tau) = 9.9\%$.

The post-pulse back flux value is particularly important for comparison of the experimental data with numerical results obtained with the thermal model. Often the evaporated mass is used for such a comparison. The model only allows the determination of the mass after evaporation termination, but in experiments the mass is measured at a much longer time after the completion of cloud expansion. The resulted discrepancy of mass removal due to the post-pulse back flux can exceed 20% (Fig. 2), and its taking into account can be important for correct comparison.

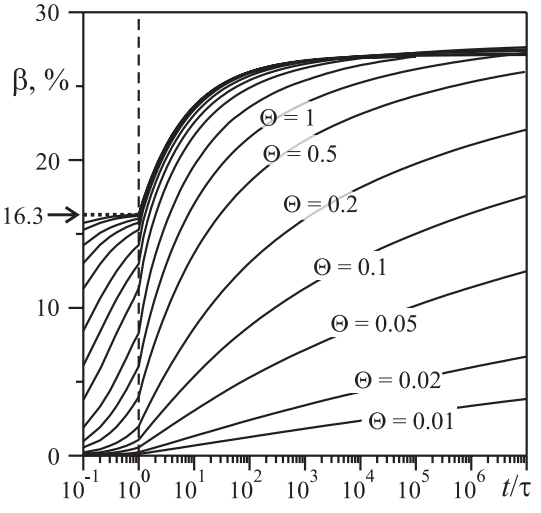

FIGURE 1 Temporal evolution of the back flux for various values of the number of evaporated monolayers $\Theta = 0.01, 0.02, 0.05, 0.1, 0.2, 0.5, 1, 2, 5, 10, 20, 50, 100, 200, 500, 1000$

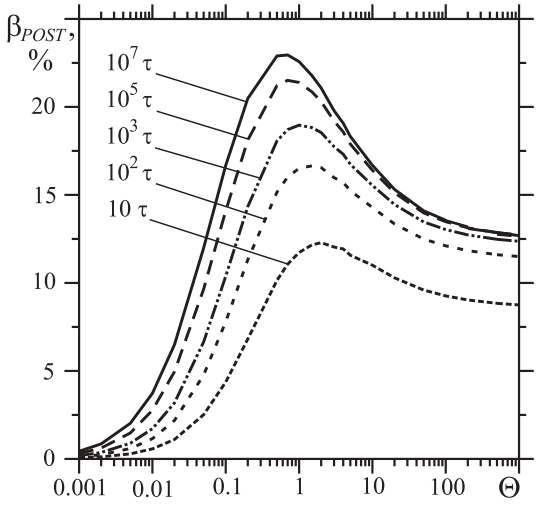

FIGURE 2 Post-pulse back flux β_{POST} as a function of the number of evaporated monolayers Θ in time moments $t = 10\tau, 10^2\tau, 10^3\tau, 10^5\tau, 10^7\tau$

3 Thermal model calculations

The obtained values of back flux were used in the thermal model of laser-induced target heating and evaporation. One-dimensional heat conduction equation is solved

$$c\rho\Big(\frac{\partial T}{\partial t} - u(T_S)\frac{\partial T}{\partial x}\Big) = \frac{\partial}{\partial x}\lambda\frac{\partial T}{\partial x} + (1 - R(T_S))\alpha I(t)\mathrm{e}^{-\alpha x} \quad (1)$$

with the boundary and initial conditions

$$T(x, 0) = T_0,\ T(0, t) = T_S(t),\ \lambda\frac{\partial T}{\partial x}\Big|_{x=0} = L_V u(T_S) \quad (2)$$

where ρ, c, λ, α are the mass density, the thermal capacity, the thermal conductivity, and the absorption coefficient of the target material; $R(T_S)$ is the reflection coefficient of the surface; $I(t)$ is the laser intensity; L_V is the latent heat for evaporation. The velocity of the surface recession is determined by the Hertz–Knudsen equation coupled with the Clausius–Clapeyron equation

$$u(T_S) = F\frac{p_b}{\rho}\sqrt{\frac{m}{2\pi k T_S}}\exp\Big[\frac{L_V}{k}\Big(\frac{1}{T_b} - \frac{1}{T_S}\Big)\Big] \quad (3)$$

where T_b is the boiling temperature under pressure p_b; $F = 1 - \beta$ is the coefficient that takes into account the back flux of particles to the surface. Melting was included into the model by using an energy accumulation technique [20].

Experiments with a graphite target [8] were chosen for verification of the model. Calculations for laser pulse duration of 13 ns (FWHM) and laser fluence in the range of $E = 1$–$8\,\mathrm{J/cm^2}$ were performed. For these conditions, absorption of laser radiation in the cloud is negligible [8], and the considered model is applicable. The latent heat of fusion 1 eV/atom was taken from [20], other properties of graphite were taken from [21]. Calculations were performed for real Gaussian shape of the laser pulse [21].

First, calculations with different values of β during evaporation without regard to the post-pulse back flux were carried out. Two limiting cases of $\beta = 0$ and $\beta = 16.3\%$ were considered. Despite the fact that the surface recession is in direct proportion to $F = 1 - \beta$, the mass removal for these cases has proved to be practically identical (Fig. 3, lines 2 and 3). This surprising result may be explained as follows: when the backscattered particles are absorbed at the surface, the surface temperature increases owing to the latent heat release. The temperature rise leads to a higher recession velocity. So, we have some self-regulating process, and the final mass removal is similar for quite different back flux values. It is worth noting that the difference in the experimental data from numerical one for $E \geq 8\,\mathrm{J/cm^2}$ (Fig. 3) is connected to laser radiation absorption in the vapor cloud that is not taken into account by the model.

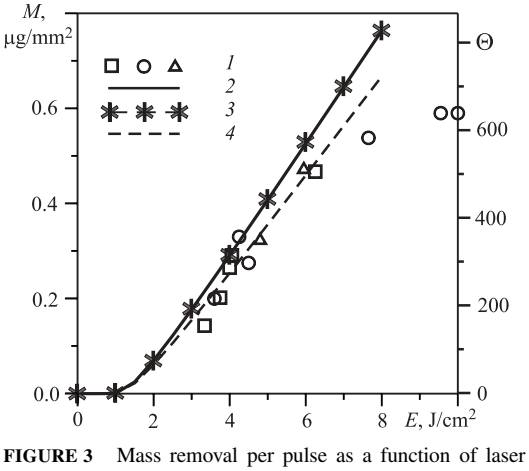

FIGURE 3 Mass removal per pulse as a function of laser fluence E for graphite target. Curve 1 corresponds to experimental data [8]; 2 to numerical data for $\beta = 0$ and $\beta_{POST} = 0$; 3 to $\beta = 16.3\%$ and $\beta_{POST} = 0$; 4 to $\beta = 16.3\%$ and $\beta_{POST} = \beta_{POST}(10^7\tau)$

At the second stage, calculations were performed for $\beta = 16.3\%$ and for the post-pulse back flux obtained for time $10^7\tau$. For any value of laser fluence E, its own value of β_{POST} was taken from the back flux calculations (Fig. 2). The resulting dependence seems to be more accurate representation of experimental points (Fig. 3, line 4).

4 Summary

On the basis of the direct Monte Carlo simulation, we obtained dependence of the back flux on the number of monolayers during evaporation and after its termination. The obtained values of back flux are substituted to the thermal model describing laser-induced solid heating with evaporation. Comparison with experimental data for graphite was performed. It is found that mass removal does not depend on the back flux value during evaporation while the post-pulse back flux consideration changes mass removal rate by 10–20% and allows a more accurate description of the experimental results.

ACKNOWLEDGEMENTS The author thanks A.K. Rebrov, M.Y. Plotnikov, and N.M. Bulgakova for useful discussions and assistance for this work.

The work has been supported by the RFBR grant (N 03-01-00213) and by the Leading Scientific School grant (N 910.2003.1).

REFERENCES

1 D. Baurle: *Laser Processing and Chemistry* (Springer, Berlin 2000)
2 P.R. Willmott, J.R. Huber: Rev. Mod. Phys. **72**, 315 (2000)
3 D. Bhattacharya, R.K. Singh, P.H. Holloway: J. Appl. Phys. **70**, 5433 (1991)
4 S. Fahler, H.-U. Krebs: Appl. Surf. Sci. **96-98**, 61 (1996)
5 J.G. Lunney, R. Jordan: Appl. Surf. Sci. **127-129**, 941 (1998)
6 T. Li, Q. Lou, J. Dong, Y. Wei, J. Liu: Appl. Surf. Sci. **172**, 356 (2001)
7 J.R. Ho, C.P. Grigoropoulos, J.A.C. Humphrey: J. Appl. Phys. **78**, 4696 (1995)
8 A.V. Bulgakov, N.M. Bulgakova: Quantum Electron. **29**, 433 (1999)
9 A. Peterlongo, A. Miotello, R. Kelly: Phys. Rev. E **50**, 4716 (1994)
10 N.Y. Bykov, G.A. Lukianov: Thermophys. Aeromech. **10**, 388 (2003)
11 R. Kelly, A. Miotello: Nucl. Instr. Meth. Phys. Res. B **91**, 682 (1994)
12 A.V. Gusarov, I. Smurov: Appl. Surf. Sci. **168**, 96 (2000)
13 G.A. Bird: *Molecular Gas Dynamics and the Direct Simulation of Gas Flows* (Clarendon Press, Oxford 1994)
14 D. Sibold, H.M. Urbassek: Phys. Fluids A **5**, 243 (1993)
15 M. Keidar, J. Fan, I.D. Boyd, I.I. Beilis: J. Appl. Phys. **89**, 3095 (2001)
16 I. Noorbatcha, R.R. Lucchese, Y. Zeiri: J. Chem. Phys. **86**, 5816 (1987)
17 D. Sibold, H.M. Urbassek: Phys. Rev. A **43**, 6722 (1991)
18 T.E. Itina, V.N. Tokarev, W. Marine, M. Autric: J. Chem. Phys. **106**, 8905 (1997)
19 N.M. Bulgakova, M.Y. Plotnikov, A.K. Rebrov: Thermophys. Aeromech. **5**, 385 (1998)
20 J. Steinbeck, G. Braunstein, M.S. Dresselhaus, T. Venkatesan, D.C. Jacobson: J. Appl. Phys. **58**, 4374 (1985)
21 N.M. Bulgakova, A.V. Bulgakov: Appl. Phys. A **73**, 199 (2001)